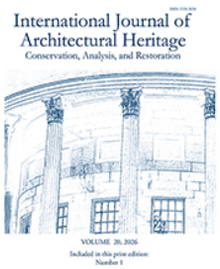

International Journal of Architectural Heritage
Conservation, Analysis, and Restoration

ISSN: 1558-3058 (Print) 1558-3066 (Online) Journal homepage: www.tandfonline.com/journals/uarc20

Assessing Salt-Induced Degradation in Historic Timber-Masonry Buildings Using Micro-Drilling: A Dutch Soda Factory Case Study

Giorgio Pagella, Silvia Naldini & Michele Mirra

To cite this article: Giorgio Pagella, Silvia Naldini & Michele Mirra (13 Jan 2026): Assessing Salt-Induced Degradation in Historic Timber-Masonry Buildings Using Micro-Drilling: A Dutch Soda Factory Case Study, International Journal of Architectural Heritage, DOI: 10.1080/15583058.2026.2615763

To link to this article: https://doi.org/10.1080/15583058.2026.2615763

INTERNATIONAL JOURNAL OF ARCHITECTURAL HERITAGE
https://doi.org/10.1080/15583058.2026.2615763

Taylor & Francis
Taylor & Francis Group

RESEARCH ARTICLE

OPEN ACCESS Check for updates

Assessing Salt-Induced Degradation in Historic Timber-Masonry Buildings Using Micro-Drilling: A Dutch Soda Factory Case Study

Giorgio Pagella [a], Silvia Naldini [b], and Michele Mirra [c]

[a]Faculty of Civil Engineering and Geosciences, Biobased Structures and Materials, Delft University of Technology, Delft, The Netherlands; [b]Faculty of Architecture, Architectural Engineering + Technology, Delft University of Technology, Delft, The Netherlands; [c]School of Architecture and Design, Structural Engineering, University of Camerino, Ascoli Piceno, Italy

ABSTRACT

The timber elements of the monumental Sodafactory building in Schiedam, the Netherlands, were investigated to assess the extent of salt-induced degradation. The damage was primarily caused by defibration, a chemical process caused by salt crystallization within the wood structure, which separates the wood cells, induces mechanical rupture, and ultimately results in a complete loss of strength. While the damage is visually detectable, it is difficult to quantify reliably. To address this, micro-drilling measurements were performed in radial and tangential direction on eight wooden beams, which appeared to be severely defibrated. Micro-drilling proved effective for quantitative measurements of decay, supported by a TU-Delft developed algorithm to scientifically determine decay from micro-drilling signals. Results showed that, beneath the layer of defibrated wood, the beams generally remained structurally sound. Only two of the eight beams were found to be severely decayed, with less than 50% of their original cross-section remaining intact. Microscopic analysis of samples from both decayed and intact areas revealed fiber separation and significant salt deposits on the beam surfaces. These findings indicate that the timber elements remain at risk, as the salt-induced decay could still progress over time, causing further degradation and increased safety risks to the historic Sodafactory building.

ARTICLE HISTORY
Received 30 September 2025
Accepted 7 January 2026

KEYWORDS
Assessment; heritage; masonry buildings; micro-drilling; salt; timber

1. Introduction

1.1. Background

The building investigated in this study is part of a former Dutch soda production factory (*Sodafabriek* in Dutch), located in Schiedam, the Netherlands, on a tract of land historically known as "Nieuwe Werk", a district positioned between the Old and New Ports. Initially developed in the early 17th century, Nieuwe Werk became an affluent residential area by the mid-18th century before transitioning into an industrial hub (Osinga-Dubbelboer 2015). The soda factory complex (Figure 1), expanded between 1883 and 1938, includes two main warehouses — Coerland and Lijfland — a mansion, and an entrance building, all facing the Schie River (Buitenhaven). These buildings are part of a monumental industrial ensemble that reflects the broader history of Schiedam, a city previously known for its jenever (Dutch spirit) production and later for its contribution to the chemical industry. The factory remained operational until 1976 and was granted municipal monumental status in 2015 (Kuipers and de Jonge 2017).

The factory refined the imported soda, dissolved it in water to form crystal soda, and processed it through crystallization, drying, and storage, primarily within the Coerland building (Kuipers and de Jonge 2017). Large iron containers installed within Coerland were used for dissolving imported anhydrous soda in water and converting it into crystal and patent soda (fine soda, obtained by mixing with sodium sulfate and centrifuging). Due to the absence of import duties on raw soda in the Netherlands during the late 19th century, it was more economical to import raw (anhydrous) soda rather than produce it locally. Although Solvay acquired the factory in 1936, it remains unclear whether the production process followed the Solvay method. The final packaging took place in Lijfland. Parts of the original silos, conveyors, and machinery remain present today, and several structural alterations, such as the removal of floors and the addition of steel supports, were made to accommodate the soda production equipment.

Both Coerland and the adjoining Lijfland warehouse display similar architectural and structural characteristics, both consisting of large, open spaces.

CONTACT Giorgio Pagella g.pagella@tudelft.nl Faculty of Civil Engineering and Geosciences, Biobased Structures and Materials, Delft University of Technology, Delft, The Netherlands

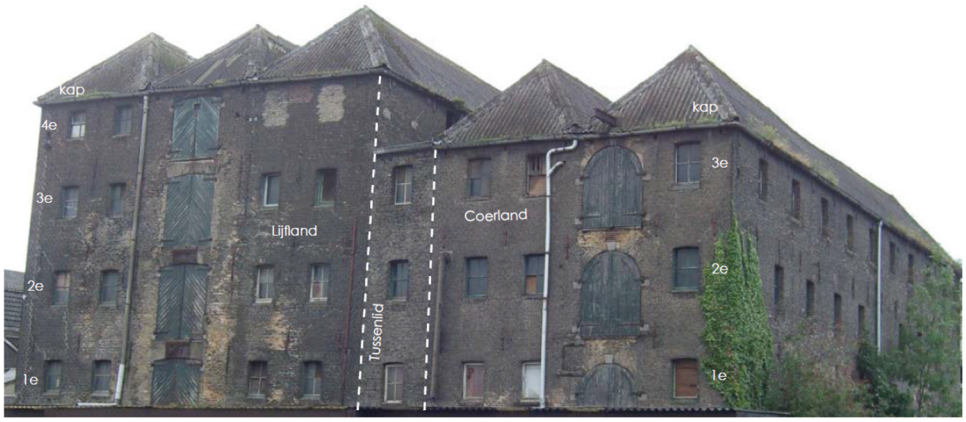

Figure 1. The 4-storeys Lijfland and 3-storeys Coerland buildings, composing the soda factory. The building complex consists of two warehouses, Lijfland and Coerland, connected by a narrow 2.1 m wide intermediate section (*Tussenlid*). Lijfland, measuring 15.3 m in height, contains three bays (4.4 m, 4.0 m, and 4.3 m) along its length and five transverse sections of 4.4 m each. Coerland (13.5 m high) is longer, narrower, and comprises two bays of 4.4 m with six transverse sections (Adaptation from Osinga-Dubbelboer 2015).

Lijfland is divided into three bays by rows of wooden columns with supporting wooden beams. The building has four columns that divide it into five spans. Coerland has five columns, dividing it into six spans (Figure 2a). The walls are built of masonry, mostly visible (uncovered). Some walls are coated with a thin layer of lime plaster. In Coerland, the ground floor walls up to the windowsills have a thicker plaster layer. The internal structure consists of wooden columns, supporting beams, and floor beams (Figure 2). The upper floors have pine wood floorboards. The ground floors in both buildings were later reconstructed in concrete, with one such intervention in Coerland dated to 1938, likely as a response to structural issues. The pine roofs of both Lijfland and Coerland share the same construction (Figure 2b), however, each building has its own roof. The roof structure consists of a horizontal beam resting on the sidewalls, anchored with wall anchors that also secure the wall plate. The wall plate is likely connected to this beam using lap joints.

1.2. Assessment of wood damage

Wood plays a crucial role in the structural composition of the Sodafabriek, as the entire load-bearing framework,

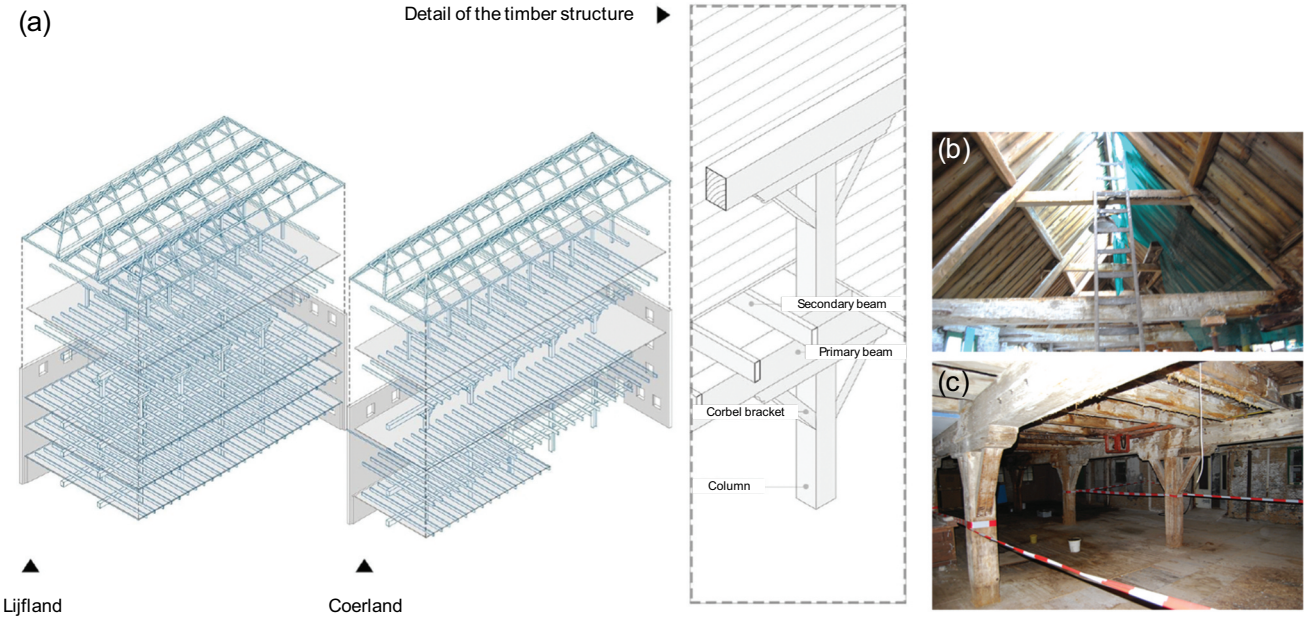

Figure 2. (a) The Lijfland and Coerland building parts of soda factory: timber elements are highlighted in blue (Adaptation from Van der Weele et al. 2020); (b) Roof structure and (c) internal timber structure in Coerland.

excluding the masonry building envelope, consists of wooden elements. Over time, these wooden components have experienced deterioration, leading to physical damage from chemical processes of salts generated by the soda production. Salts, in combination with moisture, have caused extensive, visible defibration damage throughout the building. The salt on the timber surface creates visibly white deposits known as salt efflorescence (Johnson, Ibach, and Baker 1992; Ortiz et al. 2014; Blanchette, Held, and Farrell 2002). Dissolved salts penetrate the wood, and when the wood dries, the salts crystallize inside it (Mi et al. 2020; Oren 2008). This crystallization breaks open the wood fibers (defibration), forming a "fuzzy" surface layer (Figure 3). Strong alkalis can degrade wood in a way that visually resembles fungal decay (white and bleached appearance). Initially, the damage mainly affects the surface, while the core of the wood often remains in good condition. In time, the progression of the crystallization can lead to a thinner load-bearing core of the beam, ultimately leading to failure (Figure 3b). The repeated dissolving and crystallizing process caused extensive damage also to the masonry walls of the Sodafabriek (Brocken and Nijland 2004; Sharma et al. 2025). However, this study focuses primarily on timber damage.

The second floor of the Lijfland building was used to store soda in containers, allowing it to dry and crystallize. It is highly likely that this process was the primary cause of degradation observed in the wooden elements. Water, rendered alkaline by the presence of sodium carbonate, could come into contact with the wooden beams, leading to chemical damage and accelerated deterioration of the wood. This theory helps to pinpoint a specific salt source in the building, useful for identifying the cause of the damage. Based on this assumption, selected primary and secondary beams on the ground, first, and second floors of the Lijfland building were investigated (see Chapter 2: Materials), with the choice of beams corroborated by the extensive visual defibration present, suggesting they were the most affected by moisture and salt migration. In contrast, the columns generally exhibited no visible signs of degradation, likely due to their vertical orientation.

Despite years of neglect and structural alteration, including the removal of floors and addition of steel supports next to wooden beams, the core architectural features of the factory remain. The Soda Factory complex was ultimately preserved from demolition by the intervention of the Sodafactory Cooperative, highlighting both its historical and structural value as part of the Netherlands' industrial heritage.

1.3. Scope

The objective of the study is to investigate the extent of salt-induced degradation (defibration) in eight timber beams of the historic Sodafabriek building, using micro-drilling measurements (Nowak, Jasieńko, and Hamrol-Bielecka 2016) to assess their structural condition. Light microscopy was also used to evaluate the extent of decay and to examine the condition of the material at the interface between decayed and sound wood, and identify the presence of residual salts. The investigations are carried out specifically on eight visually decayed timber beams which raise concern about the safety of the building. Micro drilling was chosen since it allows to quantify the amount of decay throughout the whole cross section of the beam, involving the utilization of a drilling tool (Eckstein and Saß 1994; Mirra et al. 2023; Nowak, Jasieńko, and Hamrol-Bielecka 2016; Pagella, Urso, Mirra, et al. 2025; Rinn 1994, 2012). A drilling needle is pushed into the material with a chosen drill and feed speed, resulting in a graphical representation of the resistance encountered during the drilling process, with the goal of measuring the thickness of the inner

Figure 3. Effect of crystallization in timber beams (a) leading to the rupture of a secondary timber beam (b) on the ground floor.

sound core of the beam (Brashaw et al. 2005; Fruehwald, Hasenstab, and Osterloh 2011; Johnstone et al. 2007; Mirra et al. 2024; Nutto and Biechele 2015; Pagella, Ravenshorst, et al. 2024). Finally, the study provides recommendations for preservation and future research.

2. Materials

The investigation focused on the primary and secondary spruce (*Picea abies*) beams located in three rooms within the Lijfland building (See Figure 4), which exhibited severe decay and raised concern about the safety of the building. The rationale behind this choice is supported by a preliminary investigation carried out using visual inspection and simple tools (chisels and screwdrivers) to remove the layer of fuzzy, decayed wood and gain a qualitative understanding of the damage severity. The selection of the analysed beams is based on the observation that the most severely deteriorated elements were located in the western part of the building (Figure 4), directly beneath the bays where the storage tanks had been placed.

At the ground floor, mid span, two secondary beams measuring 25 cm × 19 cm were tested. On the first floor, mid span, one secondary beam of the same dimensions was examined. On the second floor, first and mid span, one primary beam (38x32 cm) and four secondary beams (25 cm × 19 cm) were assessed. A summary of the investigated beams is listed in Table 1.

Table 1. List of investigated beams and their original cross-section without decay (see code reference in Figure 4).

Investigated elements	Size (height x width)	Length
GF-S02	25 x 19 cm	442.5 cm
GF-S03	25 x 19 cm	442.5 cm
FF-S01	25 x 19 cm	442.5 cm
SF-S02-1	25 x 19 cm	442.5 cm
SF-S03-1	25 x 19 cm	442.5 cm
SF-S02-2	25 x 19 cm	392.5 cm
SF-S03-2	25 x 19 cm	392.5 cm
SF-P06	38 x 32 cm	440.0 cm

3. Methodology

3.1. Micro-drilling measurements

Two micro-drilling measurements were performed through the cross-section of each investigated beam, perpendicularly to each other, and at 0.5 m of interval along the beam, to map the degradation along the beams (Brashaw et al. 2005; Gard and Van de Kuilen 2018; Nowak, Jasieńko, and Hamrol-Bielecka 2016; Pagella, Struik, et al. 2024). The rationale for performing only two measurements was to evaluate the feasibility of assessing salt-induced decay in timber beams using micro-drilling. With two measurements, it is already

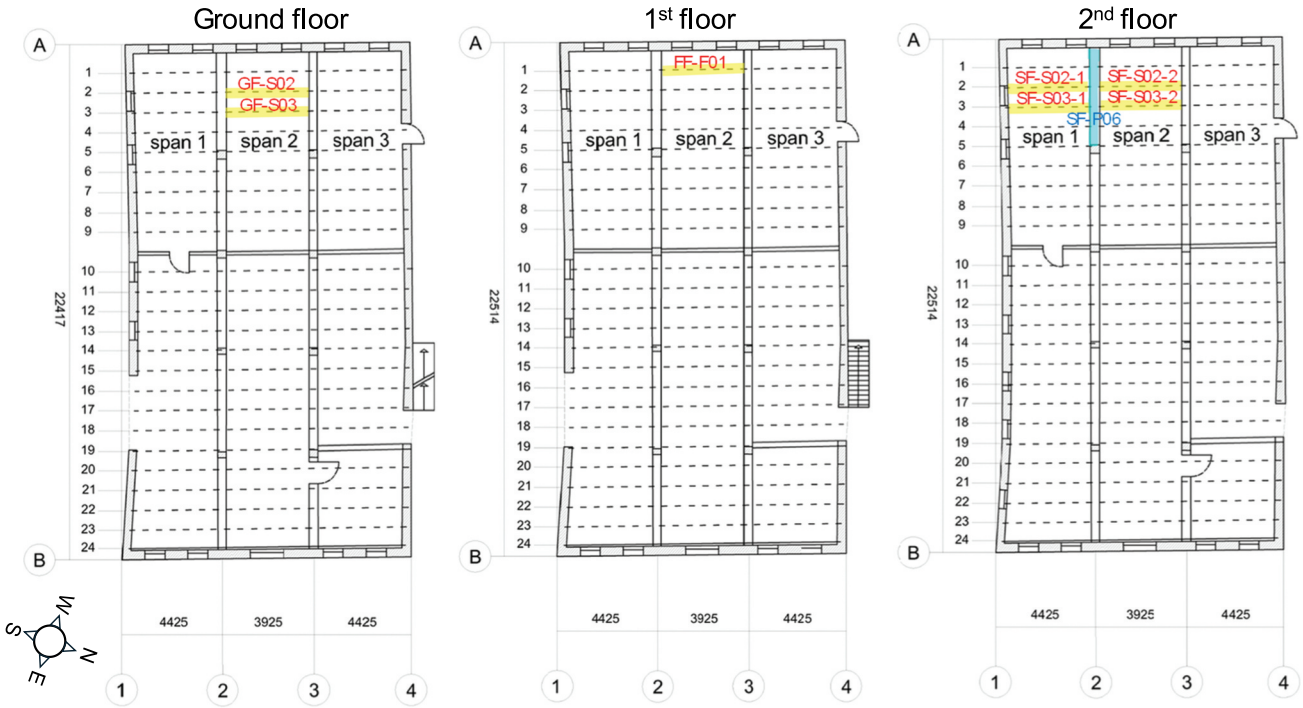

Figure 4. Plan of the ground, 1st and 2nd floors in Lijfland building, divided into 3 main spans. The beams investigated are highlighted and coded. The measurements are expressed in millimeters. The beam sections highlighted in the figure represent the original cross section without decay as listed in Table 1.

possible to obtain a quantitative estimation of the decayed material, under the assumption that decay is relatively uniform in both the radial and tangential directions of the cross-section. However, for future investigations, additional micro-drilling measurements could be performed to enhance precision and to achieve a more detailed mapping of decay around the entire cross-section. The IML-RESI PowerDrill 400 was used (IML, 2024) as shown in Figure 5a and b, produced by the German company Instrumenta Mechanik Labor System (IML). Each drill bit has a hard chrome coating with a length of 400 mm, a diameter of 1.5 mm and a 3.1 mm wide triangular shaped drill point.

Notably, moisture contents revealed to have no influence on the detection of decay, as previously demonstrated in Mirra et al. (2023). The micro-drilling signal can give information on wood annual rings (Ross 2021): maximum amplitudes correspond to latewood rings; minimum amplitudes represent early-wood (Figure 5c). Isolated high or low peaks can be often associated to wood knots and other high density anatomical variation, such as compression wood (Kollmann and Côté 1968), resulting in higher drilling amplitudes, and piths and cracks creating voids through which the drilling tool records zero or very low amplitude (Pagella and Urso 2025). By analyzing the micro-drilling signal, it is possible to observe the parts with the lowest amplitude and estimate the degraded length of the beam's cross section (Mirra et al. 2025), as shown in the example in Figure 5c. Notably, the inner part of the beam can also be decayed, for example when insects dig into the wooden beam degrading its inner core (Ross 2021).

To assess decay in timber elements, micro-drilling signals were analysed with a TU Delft developed algorithm, largely presented in Pagella, Ravenshorst, et al. (2024). The purpose of the algorithm is to analyse the micro-drilling signal and to subdivide it in zones based on the signal amplitude. The algorithm is based on the differences in signal values and not on absolute values, starting from the assumption that the wood in the centre of the pile is sound. The drill was operated at a rotation speed of 2500 r/min and an advancement rate of 150 cm/min, while recording wood resistance at 0.1 mm intervals along the penetration depth. These settings were selected based on previous investigations reported in Pagella, Mirra, et al. (2024), which formed the basis for calibrating the TU Delft-developed algorithm. The algorithm computes the following steps in order to analyse the damaged areas of the signal (referred as *soft shell*), based on the drilling amplitude measured by the micro-drilling tool:

- Signal smoothing: the signal is smoothened to a Drilling Moving Average (*Drill_MA*), giving the average length of the signal between 5 mm before and 5 mm after a specific signal point. This process involves calculating the average value of the drilling amplitude (y-axis in Figure 6a) over a specific range, specifically from 5 mm before to 5 mm after a given point along the drilling depth (x-axis in Figure 6a). This results in a smoother signal by averaging fluctuations (drops and peaks).
- Reference for sound wood: An Incremental Outwards Moving Average (IOMA) is calculated from the pile centre outwards. The maximum IOMA value on each side is considered the reference for sound wood.
- Zone classification: From the maximum IOMA value on each side of the signal, 4 zones are determined through chosen ratios between the regular Moving Average of the signal and this maximum value of the IOMA Specifically, from the outer surface inward, four zones are defined where the Drill MA reaches 20%, 40%, 60%, and 80% of the side's IOMA maximum.
- Soft shell depth: The degraded layer is identified as a sum of selected zones (zones 1 + 2), calibrated for decayed round wood in Pagella, Ravenshorst, et al.

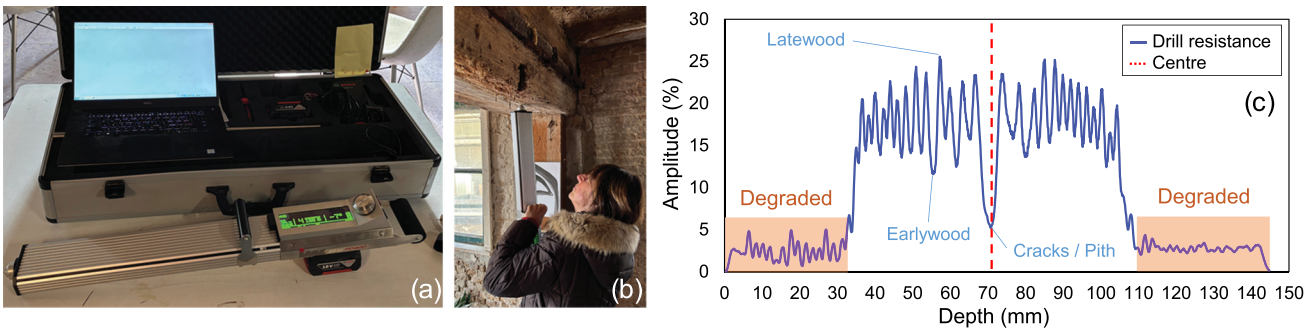

Figure 5. (a) micro-drilling IML-RESI PowerDrill 400; (b) micro-drilling measurement on a wooden beam; (c) example of a drilling measurement (drill resistance) for wood damage inspection.

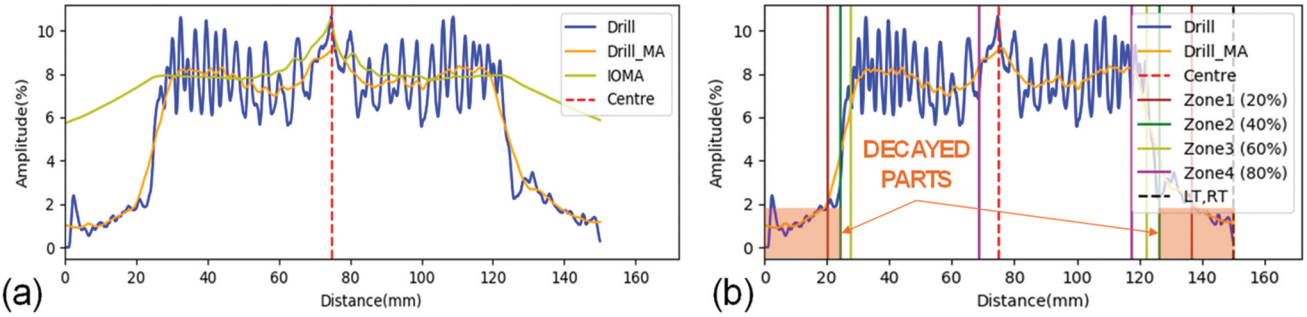

Figure 6. Example of the analysis of the drilling signal (Drill B) for a decayed spruce round wood: a) drilling moving average (Drill_ma) and IOMA from which the zones are calculated; (b) 4 zones and decayed parts (soft shell) associated to zones 1 and 2.

(2024). Both soft shell depths (right and left) are measured. An example is shown in Figure 6.

Several micro-drilling measurements were performed along the investigated beams, approximately 50 cm apart, to map the degradation continuously and avoid localized measurements that could increase the margin of error. Particular attention was given to the mid-span of the beams, where the bending moment is highest and the beams are therefore most susceptible to failure if the remaining sound, load-carrying portion is reduced due to decay.

The algorithm developed by TU Delft for analyzing micro-drilling signals provides a quantitative estimation of the soft, decayed outer layer of timber. Therefore, the novelty of this research does not lie in the micro-drilling measurements themselves, which are already widely used, but in the utilization of micro-drilling and its signal analysis that allows these measurements to shift from a qualitative to a quantitative assessment of decay.

It should be noted that the TU-Delft developed algorithm is calibrated based on a statistical analysis of a large database of 201 round softwood specimens, as reported in Pagella, Ravenshorst, et al. (2024). Specifically, it was originally developed for round piles in Amsterdam that had undergone bacterial decay. Similar to bacterial decay, salt-induced degradation primarily affects the outer layer of the timber, resulting in the complete loss of strength only in the decayed portion, while the inner core remains sound. Thus, it is reasonable to assume that said algorithm can be applied in this context as well, since the same wood species is analysed, spruce (*Picea abies*), with a decay pattern that leads to complete strength loss, and affects the outer part of the timber surface. Therefore, similar amplitude can be recorded with micro-drilling, specifically, very low in the outer layers and sound in the core volume of the spruce element. In addition, research by Mirra et al. (2023) showed that, for both sound and decayed wood, the moisture content does not affect the functioning of micro-drilling measurements or the qualitative pattern of the resulting signals. Moisture only influences the absolute amplitude of the signal — since penetrating dry wood requires more power — while the relative difference in resistance between decayed (softer) and sound (denser) wood remains consistent.

Regarding the difference in timber geometry, from round timber to beams with rectangular cross-sections, the distribution of sapwood and heartwood can vary significantly. In round timber, sapwood is generally distributed evenly around the cross-section (Kollmann and Côté 1968), whereas in beams, sapwood may be located randomly depending on how the beam was sawn and processed from the log. This variation could influence how salt degradation spreads within the beam; however, this aspect was not investigated in the present study. Concerning the applicability of micro-drilling and the TU Delft-developed algorithm, there is no reason to suggest that the rectangular geometry of the beams would affect the calculation of the remaining sound core area, since the method is primarily sensitive to the local material properties along the drilling path. The algorithm evaluates the resistance profile of the wood to detect the decayed outer layer, which is independent of the overall cross-sectional shape. As long as the drilling penetrates through the decayed surface and into the intact timber, the estimation of the sound core remains reliable.

3.2. Light microscopy observations

Light microscopy observations were also conducted to evaluate the extent of salt-induced decay and to examine the condition of the material at the interface between decayed and sound wood. To achieve this, longitudinal sections with a thickness of 30 to 50 µm, suitable for detailed microscopic analysis, were carefully prepared from the same locations where micro-drilling measurements had been performed. These thin sections allowed for a close inspection of the material, the distribution of

salt deposits, and damage caused by crystallization processes (Ortiz et al. 2014). The sections were then examined using a Keyence VHX-6000 digital microscope, which provided high-resolution images of both the wood integrity and salt-related deterioration.

4. Results

4.1. Assessment of the salt-induced decay on timber elements

In the case of the Lijfland building, which functioned as a soda factory from 1883 to 1976, alkaline degradation was caused by sodium carbonate that was used and stored on the second floor. Water transported the salts into the wooden beam causing salt crystallization and, over time, led to defibration and loss of structural integrity.

Micro-drilling measurements were performed in the radial (micro-drilling A) and tangential (micro-drilling B) directions of the cross section of the beams under investigation (see Chapter 2), and the results are summarized in Table 2. The analysis was conducted according to the procedure described in Paragraph 3.1. The assumed remaining sound cross-sectional area is calculated on the basis of two individual micro-drilling measurements. Small variations in the measurements could occur if micro-drilling were performed consistently along the entire length or thickness of the beam in multiple spots. However, for the purposes of this study, an approach based on two orthogonal micro-drilling measurements is proposed, which is based on the assumption that decay is equally distributed along the radial and tangential direction of the beam. Additional precision can be achieved by performing additional measurements.

Two detailed examples of timber beams GF-S02 and SF-S03-2 are presented in Figures 7 and 8, respectively, together with the corresponding micro-drilling signals. For the other elements, Table 2 provides a visual representation of the remaining sound portions, while the other micro-drilling signals are omitted to keep the paper concise. The analysis showed that the most decayed beams were located in the mid-span of the Lijfland building, correspondent to the building bay used to store soda in containers. In the first span, the investigated beams on the 2nd floor (SF-02–1 and SF-02–2 in Figure 9a) retained over 90% of their sound cross-sectional area. This observation is consistent with the visual inspection, which showed that the most pronounced signs of decay were mainly confined to the secondary beams in the middle bay of the building, particularly on the north side (Figure 11).

The decayed regions were primarily concentrated in the top portion of the beams, corresponding to the upper part of the radial micro-drilling measurement (right side of signal A). This is likely due to the top of the beam being in contact with the floor's transversal purlins, where moisture could accumulate more than in other areas. The limited ventilation at this interface would further promote moisture retention, facilitating the transport of salts and accelerating crystallization within the beam. The micro-drilling assessment in the tangential direction generally indicated lower decay compared to the radial direction, limited to approximately 3 cm. An exception was observed in beam SF-S03-2, where a decay depth of 78.5 mm was measured on the right side. This is shown in Figure 9b, which also illustrates a precautionary steel beam placed adjacent to the test beams. Notably, the high radial decay can likely be attributed to the beam's position directly above the soda tanks, where damage was more extensive. Finally, the micro-drilling analysis of primary beam SF-P06, which showed very limited signs of deterioration (Figure 9c), confirmed the absence of relevant decay within the beam. Micro-drilling demonstrates its effectiveness in measuring wood decay in the Sodafabriek. Especially in the case of extensive decay, when a portion of the beam is largely covered by defibrated wood, it would be difficult to accurately estimate the depth of damage without quantitative techniques such as micro-drilling.

Table 2. Results of the micro-drilling assessment on the eight investigated beams, soft shell values in radial and tangential directions and percentage of remaining sound cross-sectional area compared to the total area of the beam.

		Soft shell Radial (mm)		Soft shell Tangential (mm)		
Investigated timber beams	Location in the building	left	right	left	right	Remaining sound cross-sectional area (%)
GF-S02	Ground floor	0	100	5	35	40
GF-S03		0	71	27	13	53
FF-S01	First floor	13	32	7	8	72
SF-S02-1	Second floor	0	6	2	0	97
SF-S02-2		6	6	3	4	91
SF-S03-1		0	27	16	0	81
SF-S03-2		13	50	8.5	78.5	41
SF-P06		0	0	0	0	96

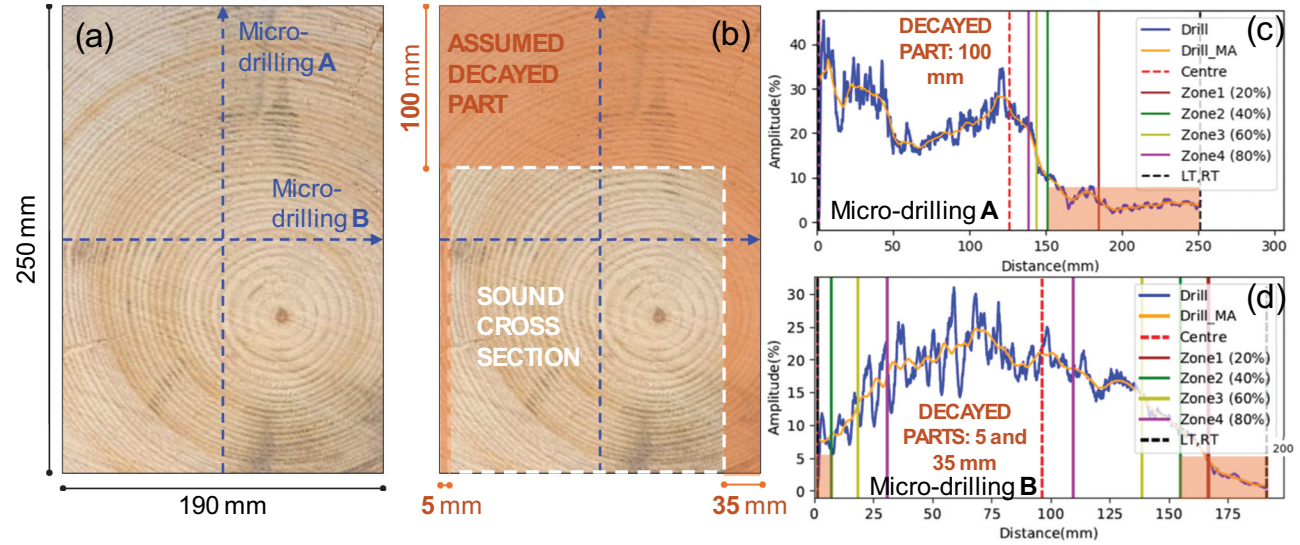

Figure 7. Decay assessment with micro-drilling: (a) cross section of the beam (example with secondary beam GF-S02) and relative micro-drilling measurements A and B. (b) Assumed decay part of the cross section based on decayed parts measured radially with micro-drilling A (c) and tangentially with micro-drilling B (d). The areas in orange represent the assumed decayed parts of the spruce beam, based on micro-drilling measurements.

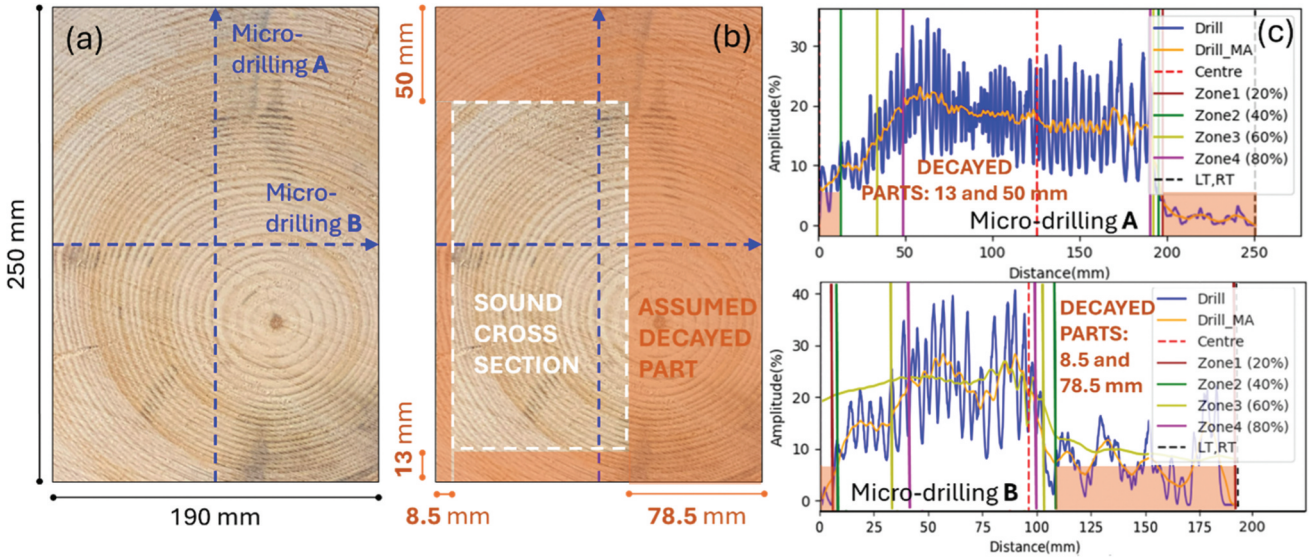

Figure 8. Decay assessment with micro-drilling: (a) cross section of the beam (example with secondary beam SF-S03-2) and relative micro-drilling measurements A and B. (b) Assumed decay part of the cross section based on decayed parts measured radially with micro-drilling A (c) and with tangentially with micro-drilling B (d). The areas in orange represent the assumed decayed parts of the spruce beam, based on micro-drilling measurements.

Notably, no fungal presence was observed in the investigated beams of the Lijfland building, likely due to the high salt content (Ortiz et al. 2014). It should be noted that not all beams in the building were assessed. Therefore, fungal decay in timber elements in other parts of the building cannot be excluded a priori. The absence of fungal growth in the examined beams can be attributed to the elevated salt concentrations within the wood (Kirker, Zelinka, and Passarini 2016). High salt content generally limits water availability and imposes osmotic stress on fungal cells, inhibiting their growth (Blomberg and Adler 1993). While this effect is not universal for all fungi, it is sufficient to prevent the development of many common wood-rotting species, as in the case of the wooden beams present in this building.

An indoor relative humidity of approximately 80–90% and a temperature of around 13°C were approximately measured during the assessment carried out in March 2025. These humidity conditions are not optimal

Figure 9. (a) beams assessed at the 2nd floor of Lijfland building, in the first span showing limited signs of defibration. (b) beams located on the 2nd floor in the mid bay, showing extensive signs of defibration. (c) detail of the connection between masonry wall and primary beam SF-P06.

for maintaining wood in a dry and sound state, where typical moisture content for indoor healthy spruce is about 11–12% (Ross 2021). As the building is unheated, the relative humidity is expected to vary significantly throughout the year, which may further influence the moisture equilibrium in the wooden elements.

It should be noted that the residual performance of the undamaged portion of the beam was not assessed but assumed to be sound. Ultimately, bending tests should be conducted to quantify the residual bending properties of these areas, which may have degraded over time due to factors such as increased stress resulting from the reduced load-carrying area.

4.2. Microscopy analysis

Several samples were taken from the beam SF-S03-1, which presented extensive signs of defibration. The samples were viewed under the microscope, according to paragraph 3.2, in order to check the presence of residual salts and provide a picture of the defibrated wood fibers.

Figure 10a shows a wood sample extracted from a sound portion of the outer surface of the analysed beam. The fibers appear compact, with crystalline deposits visible along the cell walls, suggesting localized salt accumulation. Figure 10b shows the surface of a defibrated sample, where extensive fiber separation and defibration indicate advanced mechanical rupture of the wood cell structure (Johnstone et al. 2007; Kirker, Zelinka, and Passarini 2016). The corrosive actions of the salt degraded the middle lamella causing wood cells to separate (Ortiz et al. 2014), ultimately leading to long fibers well separated from each other as visible in Figure 11b.

Finally, Figure 10c illustrates a sample taken directly beneath the defibrated wood layer, after the removal of the decayed fuzzy part, in a zone where the beam

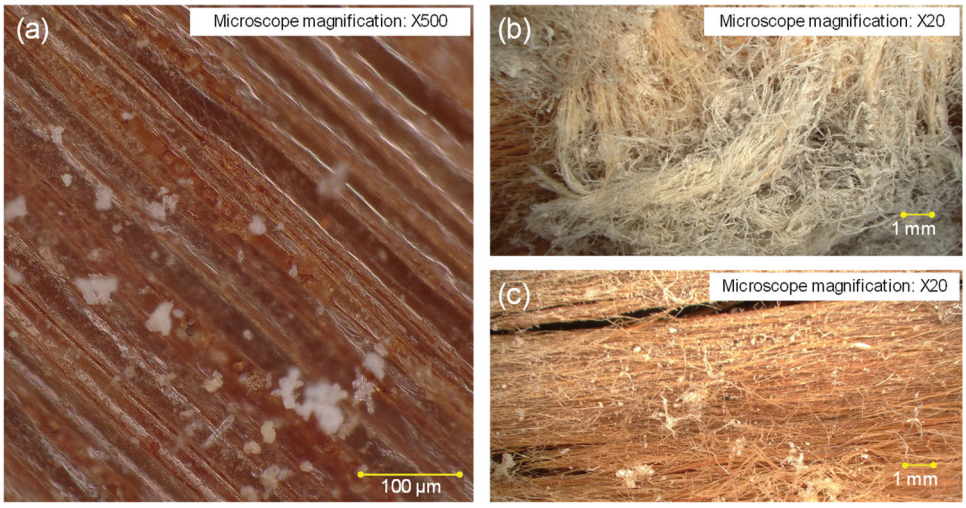

Figure 10. Microscopic views of wood samples from beam SF-S03-1: (a) sound sample taken from the beam's outer layer. At 500× magnification, the fibers appear compact, with crystalline deposits along the cell walls, indicating localized salt accumulation. (b) Defibrated samples. At 20× magnification, the surface exhibits extensive fiber separation and defibration. (c) Sample taken below the defibrated part of the beam. At 20× magnification, the fibers appear intact, presenting residuals of defibrated wood tissue and scattered crystalline deposits.

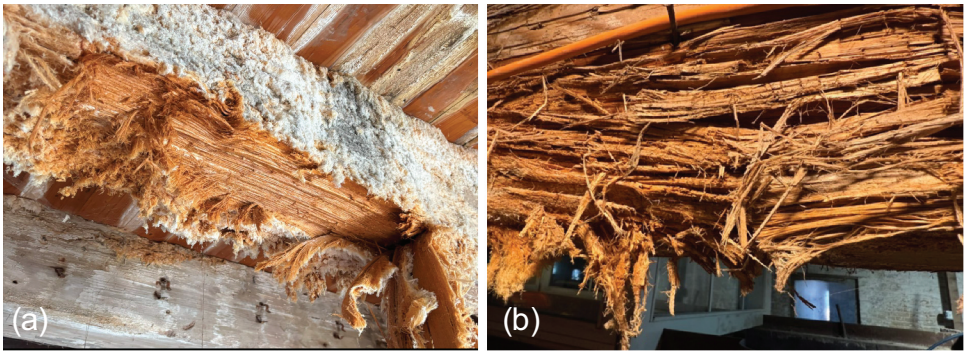

Figure 11. Salt-induced damage leading to: (a) defibrated outer surface of the timber beam, while beneath the fuzzy, decayed layer, the wood structure appears intact; (b) long wood fibers, well separated from each other, between the white salt deposits on the beam.

appeared visually intact. Here, the fibers are better preserved than in Figure 10b, although slight defibration and scattered crystalline deposits remain, representing a boundary part where the defibration started.

These observations align with the micro-drilling results, confirming that defibration and decay are mainly concentrated in the beam's outer layers. Beneath the degraded surface, the wood is less decayed and retains a uniform structure (Figure 11a), suggesting that much of its load-bearing capacity is preserved. Nevertheless, the significant presence of salt on the wood surface indicates a continuing risk: if exposed to high moisture levels, these salts could possibly reactivate, promoting ongoing decay.

5. Discussions

The historic Sodafabriek building in Schiedam, the Netherlands, exhibited extensive salt-induced damage resulting from former soda production. Water containing dissolved salts was absorbed into the timber; as moisture evaporated, salt concentrations increased at the surface, initiating corrosive chemical reactions, particularly in the middle lamella, the region bonding the wood cells. This process led to progressive cell separation and structural weakening. When the salts crystallize within the wood, the crystallization fractures the fibers, causing a decay process called *defibration*. The extent of this damage was assessed through micro-drilling measurements, which quantified the amount of decay within the beams.

In the Lijfland building, which operated as a soda factory between 1883 and 1976, alkaline degradation was caused by sodium carbonate released from the soda containers stored on the second floor, which dried and crystallized over time. Water transported these salts into the timber beams, where evaporation promoted salt crystallization and long-term defibration. This explanation is supported by the observation that the most severely decayed beams were found on the ground, first, and second floors, directly beneath the bays where the storage tanks were located.

In total, eight wooden beams were measured with micro-drilling to assess the extent of decay and estimate their remaining sound cross section. Micro-drilling revealed that, beneath the defibrated outer layers, the timber core remained largely intact. However, severe degradation was observed in particular on one ground floor beam (GF-S02) and one second floor beam (SF-03–2), where more than 50% of their cross-section was decayed. The defibration phenomenon was often located on the upper part of the beam, in contact with the transversal purlins of the floor, possibly because of the poor ventilation and residual moisture accumulating at the interface between beams and floor. While visual inspection could detect the presence of decay, visually assessing its depth was very difficult. Micro-drilling proved effective for quantitative measurements of decay, supported by the scientific methodology for interpreting micro-drilling signals as developed by Pagella, Mirra, et al. (2024) and described in paragraph 3.1. Although the algorithm was originally developed for round softwood piles with bacterial decay, it is applicable to rectangular beams because salt-induced decay similarly degrades mostly the outer layer, and the drill can detect the transition from decayed to sound wood, which is consistently different in terms of drilling resistance. Microscopy was used to confirm the presence and extent of decay. These observations were used to validate the efficiency of the algorithm for this specific type of salt-induced defibration, linking signal changes in micro-drilling to actual decayed regions.

However, the impact of salt degradation on sapwood and heartwood was not studied in this paper. Their distribution can vary significantly within timber beams, where sapwood may be located randomly depending on how the beam was processed from the

log. This variation could influence how salt degradation spreads within the beam and it should be addressed in further research.

Beneath the decayed areas of the beams, the timber structure appeared intact, as revealed by microscopy analysis, which was conducted qualitatively to assess the extent of defibration and to observe the condition of the material at the interface between decayed and sound wood. Microscopy observations also revealed a significant presence of salt on the beam surfaces. This indicates that the Sodafabriek remains at risk, especially if exposed to high moisture levels, as these salts could potentially reactivate, promoting ongoing decay and further degradation. Over time, this could lead to additional structural issues and increased safety risks.

Although soda production has ceased, residual salt deposits in the beams continues to pose a threat if moisture infiltrates or with high moisture content in the building. Sources of water ingress, including large roof openings and moisture raising damp at the wall-beam interface, should be addressed. Recommended measures include making sure that the roof is well isolated, preventing rainwater penetration, and removing salt from the wood surfaces.

Finally, it should be noted that no bending tests were carried out to quantify the residual bending properties of the sound portions of the investigated beams, which may have degraded over time due to factors such as increased stress on the beams caused by the reduced load-carrying area. While the present study focused exclusively on timber, the condition of the masonry was not assessed. Future investigations should also evaluate damage to the masonry elements to provide a comprehensive understanding of the building's structural integrity.

These topics represent valuable avenues for further research, where micro-drilling measurements can be used to assess the depth of salt-induced decay in timber and evaluate the remaining sound cross-section of structural elements. In cases like the one presented in this paper, decay may appear severe, widespread, and difficult to assess visually. However, the micro-drilling results showed that, despite extensive fuzzy-decayed surfaces caused by salt damage, the underlying timber often remained intact, indicating good preservation of the wood.

Such findings can inform future preservation and management strategies for timber structures. Micro-drilling provides quantitative data that is relatively easy to collect, as the inspection requires only a drilling tool. The process is fast, and, when combined with the signal analysis algorithm developed by TU Delft, it can deliver reliable information to support decision-making regarding the conservation of timber elements.

6. Conclusions

In conclusion, the following aspects were found in this study:

(1) The most degraded timber beams in the Sodafabriek were located beneath former soda containers, used for dissolving imported anhydrous soda in water and converting it into crystal and patent soda. Water containing dissolved salts was absorbed into the timber, causing corrosive chemical reactions, particularly in the middle lamella, the region bonding the wood cells. This process led to wood defibration: a progressive cell separation and structural weakening exacerbated by poor ventilation, residual moisture, and salt accumulation at beam-floor interfaces.
(2) By using micro-drilling measurements combined with the TU Delft-developed algorithm, the extent of decay in eight timber beams of the Sodafabriek building was successfully quantified. The integration of micro-drilling with the algorithm enables a shift from a qualitative to a quantitative assessment of decay, and the novelty of this approach lies in this quantitative capability.
(3) Results showed that while the outer layers of the beams exhibited extensive decay, the inner timber cores often remained structurally intact. In two beams, however, more than 50% of the cross-section was severely degraded. The defibration damage was often more severe on the upper side of the beams, at the interface with the transversal purlins of the floor, likely due to poor ventilation and the accumulation of residual moisture in this area.
(4) Microscopy confirmed the presence of salt deposits on beam surfaces, indicating a continuing risk of reactivation and further decay under high moisture conditions. This was important to validate the micro-drilling for this specific type of salt-induced defibration, connecting signal changes in micro-drilling to actual decayed regions.
(5) Preventive interventions are recommended, including improving roof isolation to avoid water ingress, and removing surface salts on timber beams to limit further defibration damage.
(6) Evaluation of the residual bending strength of the decayed timber beams, as well as the condition of the masonry elements, are recommended, as these aspects were not addressed in the present study and will be the subject of future investigations.

Acknowledgement

The authors gratefully acknowledge the Sodafabriek management team for granting access to the structure, as well as the master's students of TU Delft Architecture for their collaboration on this project.

Disclosure statement

No potential conflict of interest was reported by the author(s).

Funding

No funding was received for this work.

ORCID

Giorgio Pagella http://orcid.org/0000-0002-2552-4877
Silvia Naldini http://orcid.org/0000-0002-2969-3803
Michele Mirra http://orcid.org/0000-0002-9898-8971

References

Blanchette, R. A., B. W. Held, and R. L. Farrell. 2002. "Defibration of Wood in the Expedition Huts of Antarctica: An Unusual Deterioration Process Occurring in the Polar Environment." *Polar Record* 38 (207): 313–322. https://doi.org/10.1017/S0032247400018003.

Blomberg, A., and L. Adler. 1993. "Tolerance of Fungi to NaCl. Stress Tolerance of Fungi." *Mycology Series* 10, ISSN 0730-9597, 209–231.

Brashaw, B. K., R. J. Vatalaro, J. P. Wacker, and R. J. Ross. 2005. *Condition Assessment of Timberbridges: 1. Evaluation of a Micro-Drilling Resistance Tool. Gen. Tech. Rep. FPL-GTR-159*. Madison,WI: U.S. Department of Agriculture, Forest Service, Forest Products Laboratory. 8.

Brocken, H., and T. G. Nijland. 2004. "White Efflorescence on Brick Masonry and Concrete Masonry Blocks, with Special Emphasis on Sulfate Efflorescence on Concrete Blocks." *Construction and Building Materials* 18 (5): 315–323, ISSN 0950-0618, https://doi.org/10.1016/j.conbuildmat.2004.02.004.

Eckstein, D., and U. Saß. 1994. "Bohrwiderstandsmessungen an Laubbäumen Und ihre holzanatomische Interpretation (Wood Anatomical Interpretation of Resistance Drilling Profiles from Broad Leaf Trees)." *Holz als Roh-und Werkstoff* 52 (5): 279–286. https://doi.org/10.1007/BF02621413.

Fruehwald, K., A. Hasenstab, and K. Osterloh. 2011. "Detection of Fungal Damage of Wood in Early Stages Using Drilling Cores and Drilling Resistance Compared to Non-Destructive Testing Methods: SHATIS." In Proceedings of the 11th International Conference on Structural Health Assessment of Timber Structures (SHATIS), edited by José Saporiti Machado, Jorge M. Branco, and Paulo Lourenço, Lisbon, Portugal, June.

Gard, W. F., and J. W. G. Van de Kuilen. 2018. "Micro-Drilling Resistance Measurements of Dense Hardwoods for Hydraulic Structures." In *WCTE - World Conference on Timber Engineering*, Seoul, South-Korea.

Iml. Accessed March 19, 2024. https://www.iml-service.com/product/iml-powerdrill/.

Johnson, B. R., R. E. Ibach, and A. J. Baker 1992. "Effect of Salt Water Evaporation on Tracheid Separation from Wood Surfaces." *Forest Products Journal* 42 (7/8): 57–59.

Johnstone, D. M., P. K. Ades, G. M. Moore, and I. W. Smith. 2007. "Predicting Wood Decay in Eucalypts Using an Expert System and the IML-Resistograph Drill." *Arboriculture & Urban Forestry* 33 (2): 76–82. https://doi.org/10.48044/jauf.2007.009.

Kirker, G., S. Zelinka, and L. Passarini. 2016. "Avast Ye Salty Dogs: Salt Damage in the Context of Coastal Residential Construction and Historical Maritime Timbers." In *Conference 112th Annual meeting of the American Wood Protection Association*, Sand Juan, PR.

Kollmann, F., and W. A. Côté. 1968. *Principles of Wood Science and Technology*, 592. Vol. 1. Berlin, Heidelberg: Springer-Verlagp, ISBN 978-3-642-87930-2.

Kuipers, M., and W. de Jonge. 2017. *Designing from Heritage: Strategies for Conservation and Conversion*. Delft: Heritage & Architecture.

Mi, X., T. Li, J. Wang, and Y. Hu. 2020. "Evaluation of Salt-Induced Damage to Aged Wood of Historical Wooden Buildings." *International Journal of Analytical Chemistry* 2020:1–11. https://doi.org/10.1155/2020/8873713.

Mirra, M., G. Pagella, W. F. Gard, G. J. P. Ravenshorst, and J. W. G. van de Kuilen. 2023. "Influence of Moisture Content on the Assessment of Decay Levels by Micro-Drilling Measurements in Wooden Foundation Piles." World Conference on Timber Engineering, Oslo, Norway.

Mirra, M., G. Pagella, W. Gard, G. Ravenshorst, and J. W. van de Kuilen. 2025. "Safeguarding Amsterdam's Heritage: Predicting Sapwood Width to Preserve Ancient Wooden Foundations." *Wood Material Science & Engineering* 20 (5): 1128–1130. https://doi.org/10.1080/17480272.2025.2509811.

Mirra, M., G. Pagella, M. Lee, W. Gard, G. Ravenshorst, and J. W. G. van de Kuilen. 2024. "Characterisation of Bacterial Decay Effects on Wooden Foundation Piles Across Various Historical Periods." *Construction and Building Materials* 421:135670. https://doi.org/10.1016/j.conbuildmat.2024.135670.

Nowak, T. P., J. Jasieńko, and K. Hamrol-Bielecka. 2016. "In Situ Assessment of Structural Timber Using the Resistance Drilling Method – Evaluation of Usefulness." *Construction and Building Materials* 102:403–415. https://doi.org/10.1016/j.conbuildmat.2015.11.004

Nutto, L., and T. Biechele. 2015. "Drilling Resistance Measurement and the Effect of Shaft Friction—Using Feed Force Information for Improving Decay Identification on Hard Tropical Wood." In Proceedings: 19th International Nondestructive Testing and Evaluation of Wood Symposium, edited by Feagri, R., 154–161. Madison, WI: U.S. Department of Agriculture. https://doi.org/10.2737/FPL-GTR-239

Oren, A. 2008. "Microbial Life at High Salt Concentrations: Phylogenetic and Metabolic Diversity." *Saline Systems* 4 (1): 2. https://doi.org/10.1186/1746-1448-4-2.

Ortiz, R., H. Navarrete, J. Navarrete, M. Párraga, I. Carrasco, E. de la Vega, M. Ortiz, P. Herrera, and R. A. Blanchette. 2014. "Deterioration, Decay and Identification of Fungi Isolated from Wooden Structures at the Humberstone and Santa Laura Saltpeter Works: A World Heritage Site

in Chile." *International Biodeterioration & Biodegradation* 86, Part C:309–316 ISSN 0964-8305, https://doi.org/10.1016/j.ibiod.2013.10.002

Osinga-Dubbelboer, E. M. 2015. *Sodafabriek: Constructie en Schadeanalyse*, MSc Thesis, in Dutch: Hogeschool Utrecht.

Pagella, G., M. Mirra, G. Ravenshorst, W. Gard, and J. W. van de Kuilen. 2024. "Characterization of the Remaining Material and Mechanical Properties of Historic Wooden Foundation Piles in Amsterdam." *Construction and Building Materials* 450, Article 138616.https://doi.org/10.1016/j.conbuildmat.2024.138616

Pagella, G., G. Ravenshorst, M. Mirra, W. Gard, and J. W. van de Kuilen. 2024. "Innovative Application of Micro-Drilling for the Assessment of Decay and Remaining Mechanical Properties of Historic Wooden Foundation Piles in Amsterdam." *Developments in the Built Environment* 19 (100514): 100514–101659. https://doi.org/10.1016/j.dibe.2024.100514

Pagella, G., M. Struik, M. Mirra, and J. W. van de Kuilen. 2024. "Small-Scale Testing of Water-Saturated Wooden Discs for Determining the Strength Properties of Timber Foundation Piles." *Wood Material Science and Engineering* 20 (3): 734–736. https://doi.org/10.1080/17480272.2024.2426070

Pagella, G., and T. Urso. 2025. "Material and Environmental Factors Impacting the Durability of Oak Mooring Piles in Venice, Italy." *Sustainability* 17 (10): 4327. https://doi.org/10.3390/su17104327

Pagella, G., T. Urso, M. Mirra, S. Naldini, and J. W. van de Kuilen. 2025. "Traditional Wooden Foundation Piles in Amsterdam and Venice: Techniques for the Assessment of Their State of Conservation." *Wood Material Science & Engineering* 2025:1–16. https://doi.org/10.1080/17480272.2025.2466104

Rinn, F. 1994. "Resistographic Visualization of Tree Ring Density Variations." International Conference Tree Rings and Environment, Tucson, AZ. Printed in Radiocarbon, 871–878.

Rinn, F. 2012. "Basics of Typical Resistance-Drilling for Timber Inspection." *Holztechnologie* 53 (2012): 3p. 24–29.

Ross, R. J. 2021. Wood Handbook Wood as an Engineering Material. *Forest Products Laboratory*. *General Technical Report FPL-GTR-282*. Madison, WI: U.S. Department of Agriculture, Forest Service, Forest Products Laboratory, p. 543.

Sharma, S., R. Esposito, A. M. D'Altri, and G. Castellazzi. 2025. "Salt Crystallisation and Weathering in Masonry Retaining Walls: A Multiphase Modelling Approach." *Journal of Building Engineering* 111:112999, ISSN 2352-7102, https://doi.org/10.1016/j.jobe.2025.112999

Van der Weele, P., S. Yu Jung Lim, H. Li Wang, and Y. Chen Shih. 2020. Sodafabriek Technical Report, AR0141 CSI Heritage. Technical Report. Delft University of Technology.